ELSEVIER

Thin Solid Films 412 (2002) 24–29

thin solid films

www.elsevier.com/locate/tsf

Shadow mask technology

T. Schallenberg*, C. Schumacher, S. Gundel, W. Faschinger

Physikalisches Institut, EP III, Universität Würzburg, Am Hubland, D-97074 Würzburg, Germany

Abstract

We investigate molecular beam epitaxy (MBE) regrowth through shadow masks developed from AlGaAs/GaAs layers on GaAs [001] substrates. Adjusting the directions of the molecular beams relative to the masks results in in situ lateral structuring. This enables us to modify doping and composition within one layer, to shift it laterally, and even to split it or to reduce its width relative to the mask's aperture. The resolution of this selective area epitaxy (SAE) technique is restricted by half shadows and surface diffusion. With diaphragms and thin masks it is possible to decrease half shadows to a few nanometers. However, diffusion mainly is a material parameter. We have investigated III–V and II–VI semiconductors. In the latter case it is extremely dependent on the crystal orientation. Along [1−10] diffusion lengths are very short. This is in agreement with ab initio calculations in our group. Thus lateral structuring with a resolution of a few nanometers is achieved. We discuss the degrees of freedom, which arise from different chamber geometries and mask concepts. With simple striped masks complex structures such as stacked three colour detectors or selective contacts to embedded 2DEGs can be realised. Three novel mask concepts will be presented. Deeply underetched masks serve as elastic substrates for misfit layers over the critical thickness without plastic relaxation. Second, as an analogy to cleaved edge overgrowth, we use masks developed from AlGaAs/GaAs superlattices. Finally interconnected structures with lateral periodicity of a few micrometers have been realised with grid masks.

Keywords: Molecular beam epitaxy; Shadow masks; Selective area epitaxy; Superlattices

1. Introduction

Mechanical shadow masking is, generally speaking, an obsolete method of patterning vacuum deposited films. However, when its limitations are unimportant, one may exploit its several advantages over modern lithographic techniques. Being an in situ technique it helps to improve device characteristics [1]. Devices, which are not feasible by post-processing or ex situ techniques, have been realised by in situ lateral structuring [2,3]. Also large-scale integration of devices has been demonstrated [4].

Usually removable mechanical masks made of refractory materials (W, Ta, Mo, and Si) are used for selective area epitaxy (SAE) [5]. Shadow masks with small apertures are realised by anisotropic etching of pyramidal shaped holes through thin (001) Si wafers (50 μm thick) [6]. Alternatively a p^+-Si or silicon nitride membrane is prepared and openings are structured by conventional lithography [7]. Both kinds of masks are used in contact mode, which means that the aperture defining side is in contact with the substrate. In this way the partial shadow width, which is proportional to the residuary shadowing distance, is minimised. Selective growth of patterned GaAs/AlGaAs such as with a width as narrow as 1 μm has been demonstrated [6]. However, when using an in situ mask fixture, which is necessary for multi-step masking, the worse contact (increased shadowing distance) causes a minimum 5–7 μm width of the mesa edges [5]. By using a relative motion between the mask and the substrate during deposition a controlled lateral variation of chemical composition in the epitaxial layer structure can be realised. The smallest width of lines written in this way is approximately 10 μm [8]. For using different in situ masks absolute positioning is an unsolved problem. In ultra-high vacuum environment a resolution of the order of several micrometers has not been realised. Due to this limited resolution and alternative SAE techniques, which realise in situ growth of small dimensional structures by means of self-assembling techniques, shadow growth with removable shadow masks has lost its importance for semiconductor technology.

*Corresponding author.

0040-6090/02/$ - see front matter
PII: S0040-6090(02)00307-3

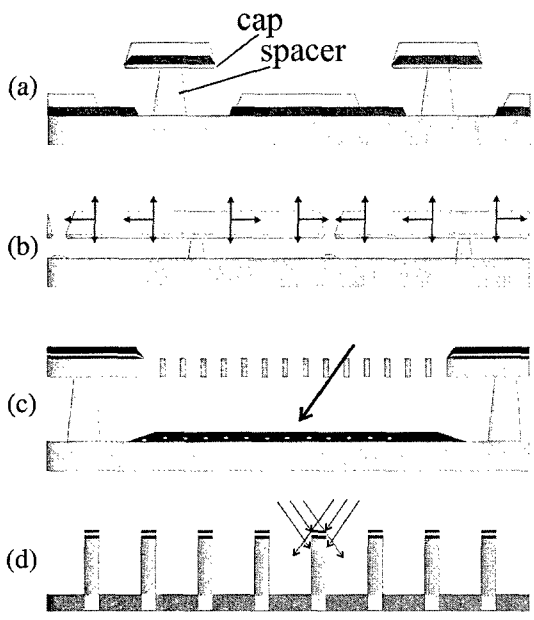

Fig. 1. (a) Growth into T-shape masks for lateral structuring. (b) Growth onto deeply underetched T-masks. The elasticity of the mask is used in order to increase the critical thickness of a misfitted layer. (c) Grid masks enable the growth of coherent structures with lateral periodicity. (d) An analogy to cleave edge overgrowth. Selectively etched SL.

2. Stationary shadow masks

We investigate molecular beam epitaxy (MBE) regrowth through shadow masks developed from AlGaAs/GaAs layers on GaAs [001] substrates (see Fig. 1a). First the GaAs cap layer is structured lithographically and subsequently underetched by hydrofluoric acid, which selectively attacks the AlGaAs spacer layer and uncovers the atomically smooth substrate surface. In this way sub-micrometer apertures and an MBE-precise distance of the shadow edge from the substrate is realised. Döhler et al. have first considered the alignment of such stationary masks relative to the incidence angles of the material sources [2,9,10]. By synchronising mask rotation with shutter operation they achieved selective doping.

2.1. Spatial resolution

Without diffusion the resolution of lateral structuring is limited only by the extend of partial shadows Δx. These are due to the finite aperture y of the oven's orifice (see Fig. 2c). For the RIBER 32 MBE (chamber geometry sketched in Fig. 2) with standard effusion cells the angular spread of the molecular beams is approximately 10°. This is minimised by an increased sample–source distance d and by using small apertures in front of the ovens. In the latter case hot-lip cells or separate heatings are required to prevent accruing of the apertures. Since the width of partial shadows Δx below the mask is proportional to the distance t from the shadow edge, we have reduced the thickness of the spacer layer in order to reduce the width of partial shadows to the order of 10 nm.

In such small dimensions controlled deposition is interfered by diffusion dynamics. For MBE of III–V semiconductors diffusion lengths of the order of several micrometers limit the shadow growth resolution. Submicrometer resolution is only realised with weak-diffusing components like Si or Al. However, dynamics are effectively reduced at low substrate temperatures (LT). Therefore magnetic III–V semiconductors, which are regularly LT-grown, are ideally suited for in situ nanostructuring with the shadow growth technique. Another important class of materials, which is ideally suited to be structured by shadow growth, is wide-bandgap II–VI semiconductors. In this case we have observed an extremely anisotropical diffusion behaviour. When ZnSe (Se-rich) is deposited through stripe-masks oriented along the [1 − 10] direction faceting of the mesa edges due to self-assembly is observed. In contrast to this a round-shape profile of the edges is observed in the perpendicular [110] orientation. This shape is due to the flux-gradient of the partial shadow. From these experiments we conclude that the preferential diffusion-direction is along [110] with diffusion lengths of the order of 1 μm, while in the perpendicular [1 − 10] direction diffusion lengths are only of the order of 10 nm. This can be understood by results obtained from density functional calculations in the local density approxima-

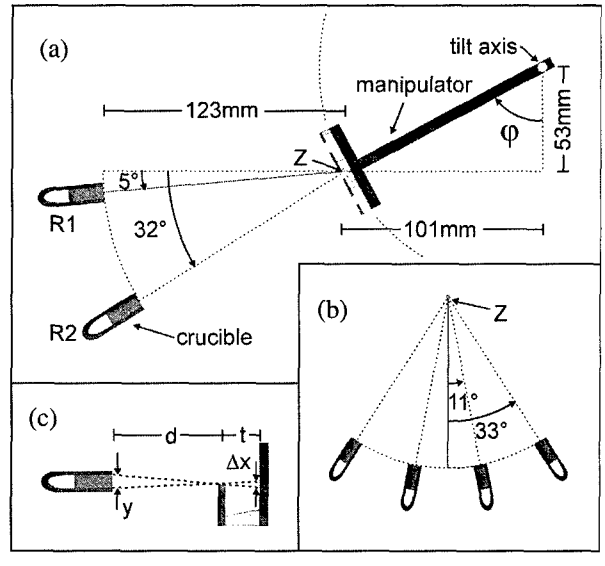

Fig. 2. (a) Sketch of the RIBER 32 chamber geometry with the manipulator in standard position (tilt angle $\varphi = 62°$). The effusion cells (not scaled) are aligned in two angles from the horizontal plane. (b) Their horizontal separation is 22°. (c) The partial shadow Δx is due to the finite aperture y of the oven's orifice.

tion. For these calculations the total energy of a single zinc atom on top of an otherwise perfect selenium-rich (2×1) surface was calculated as a function of position in order to obtain a map of the surface potential for zinc [11]. The result shows that for diffusion in [1$\bar{1}$0] direction the zinc atoms have to overcome barriers of approximately 640 meV resulting from the selenium dimer rows, whereas similar barriers in the [110] direction are only of the order of 180 meV. A more detailed discussion of diffusion dynamics during the growth of ZnSe will be given in a later contribution.

2.2. Degrees of freedom

Compared with shadow growth with removable masks, the degrees of freedom for lateral structuring with only one stationary mask are somewhat reduced. In order to compensate this deficiency we have done intense basic investigations and developed techniques, which further expand the degrees of freedom of this technique.

These are lateral layer offset, size-control, selective doping, secondary shadowing, and composition modification. Lateral layer offset is realised by changing the angle of incidence of parallel molecular beams relative to the shadow mask. In our MBE chamber pivoting the sample manipulator does this. For a shadow mask of thickness t and an incidence angle φ the absolute layer offset x is given by $x=t\tan(\varphi)$. Size control is due to enhanced compound-sticking. At the growth temperature the single elements reevaporate from the surface where they cannot find their compound partners. With non-parallel incident molecular beams growth is restricted mainly to the overlap of the molecular beams. This option depends on the sticking coefficients (material properties), and is not effective with most III–Vs (e.g. gallium does not evaporate and forms droplets where no arsenic is incident). Selective doping is realised by varying the incidence directions of the acceptor and donator molecular beams. In the same way composition modifications of mixed crystals are achieved by adding the mixing components with different angles. Finally secondary shadowing enables the deposition of laterally separated layers. By means of secondary shadow effects in situ grown steep edges can also be used instead of extremely thin shadow masks. In this way it is also possible to integrate shadow edges of different height into one structure.

With all these many degrees of freedom controlled deposition of complex nanostructures in three dimensions is realised. Structures, which demonstrate the potential of this technique, include the nipi band filling modulator (selective contacts to doping-superlattices first realised by Döhler et al. [2]), selective deposition of sub-micrometer in situ contacts to embedded layers (stapled three colour detectors or selective contacts to

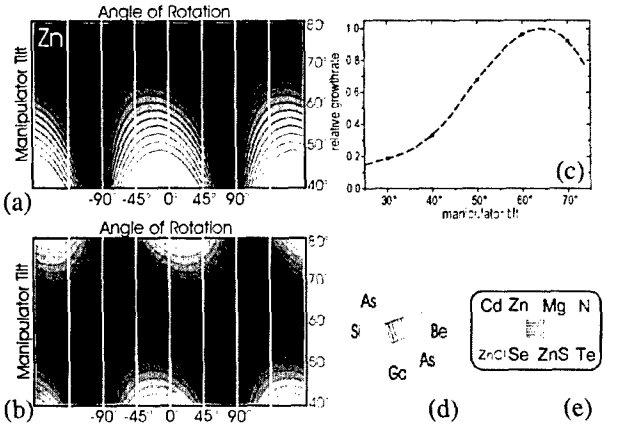

Fig. 3. Angles of incidence φ (relative to a stripe mask) dependent from manipulator tilt and rotation angles [(black) $0°\leq abs(j)\leq 50°$ (white)]. (a) Zn effusion cell (R1; left inner cell). (b) Se effusion cell (R2; left inner cell). (c) Growth rates of AlGaAs/GaAs-SLs (R2 cells) dependent on the manipulator tilt angle. (d) Center-symmetric arrangement of the effusion cells. (e) Alignment of the effusion cells in two lines.

embedded 2DEGs can be realised in this way [12]), homogeneous ZnSe quantum-wires embedded in Mg-ZnSSe [13], and ZnSe-embedded CdSe quantum-dots arrayed in a single line [14]. These structures have in common that they cannot be realised by any other method.

2.3. Chamber geometry

For the design of new devices with the above stated degrees of freedom some restrictions, which are due to the MBE chamber geometry have to be considered. As has been discussed before the resolution limiting angular spread of the molecular beams is effectively reduced with diaphragms, which minimise the apertures of the sources. Therefore the crucial restrain of the degrees of freedom is the inability to freely vary the directions of the molecular beams. In a standard MBE chamber geometries there are only two co-ordinates (manipulator-tilt and -rotation; see Fig. 3a,b) defining the possible alignments of the sample holder relative to a stationary array of elemental cells. Therefore the residual freedoms critically depend on the cells' arrangement. Chambers with a source alignment in two lines, and the center symmetrical type are commonly used (see Fig. 3d). In the second case it is not possible to align a stripe-mask in the way that more than two molecular beams are incident parallel (with respect to the stripes). Therefore uniform mixed crystals are only achieved by continuously rotating the samples, or by mixing the binary compounds digitally. This severely constrains the freedom to choose whatever material. However, in our RIBER 32 MBE chamber (see Fig. 2a,b) the sources are aligned in two lines with each four elemental cells

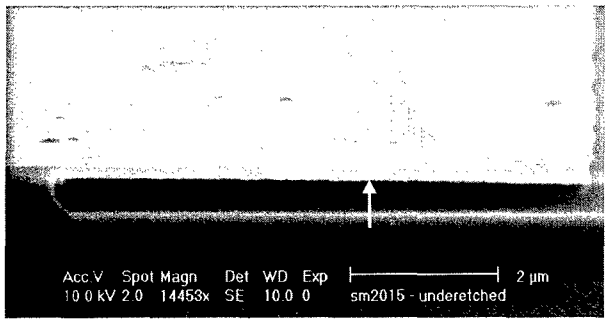

Fig. 4. Elastic mask: a deeply underetched GaAs-layer.

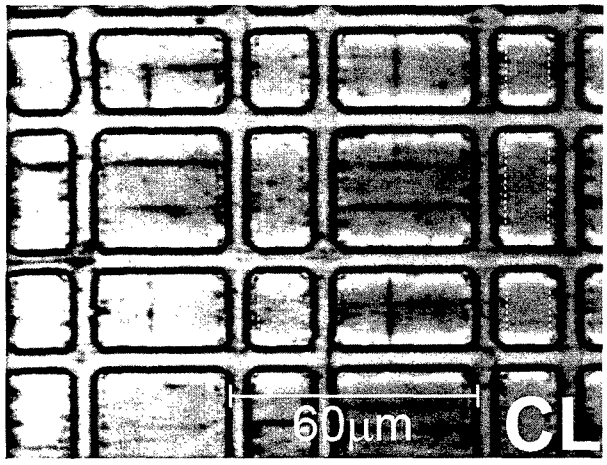

Fig. 5. Cathodo-luminescence micrograph of an overgrown elastic masks. The dashed boxes indicate not underetched areas of elastic fields, which are free of dark-line and point-defects.

(Fig. 3d). In this configuration the growth of uniform quaternary layers is possible. Pivoting the sample manipulator does offsetting the mixed-crystal layers. And non-parallel incidence of the molecular beams is possible in a wide range of the (two-dimensional) manipulator positions. Therefore a large variety of complex structures can be grown. Usage of multi-crucible cells, compound sources, or an UHV transfer system, which interconnects several MBE chambers, further expands the possibilities. In the Würzburg MBE cluster six MBE chambers plus an in situ metallization chamber are connected together in this way.

For a further improvement of the chamber geometry for directed molecular beam epitaxy the possibility to manipulate the sources' arrangement in situ is the main task. Simple solutions to this problem are valved cells with kinked line cracking zones lapping into the chamber. In situ manipulation of the outlets' position can be arranged by rotating this extension. Valved cells are generally important for this technique since the effective flux rates vary with manipulator tilt. The consequences of this are variations of the growth rates (see Fig. 3c), the composition of mixed crystals, and the critical flux-ratio of compounds (p_{II}/p_{VI}, and p_{III}/p_V, respectively) from the stoichiometric value. The final task that is important for the chamber geometry is the position of the tilt-axis. This should cross the sample, since otherwise flux variations tend to be more complex (as in the RIBER 32 MBE; see Fig. 2a).

3. Mask concepts

The interesting properties of AlGaAs/GaAs shadow masks (selectively etchable, pseudomorphic, strong, and elastic) have inspired us for the following three novel mask concepts.

3.1. Elastic mask

The first mask is based on the extreme strength and elasticity of deeply underetched GaAs-cap layers. Thin layers are even stable if the free-standing parts drag out 50 times the layer thickness h_b (Fig. 4). Such fine structures can be used as elastic substrates (see Fig. 1b). Lo [15] has calculated that the effective critical thickness t_{eff} (for the generation of misfit dislocations) of films deposited on ideal elastic substrates approaches infinity ($t_{eff}^{-1} = t_c^{-1} - h_b^{-1}$) as the substrate thickness h_b is reduced to below the critical thickness t_c (with inelastic substrate). For $t_c < h_b < 2t_c$ Lo also supposed that threading dislocation free heteroepitaxy could still be achieved, since threading dislocations tend to be pushed into the thin substrate due to the effect of image force. However, selective area epitaxy on plain substrates also expands critical thicknesses. This is due to lateral elastic relaxation of selectively deposited layer, if the thickness to width ratio $h/2l$ is high. Jain et al. have performed finite element calculations for this case, and found that for the ratios $h/2l = 0.05$, and 0.1 stresses in the middle of an elastically relaxed stripe are reduced by 26%, and 40%, respectively [16]. We have defined fields on a shadow mask by opening narrow aperture stripes along [110] and [1 −10] direction. The edges of these fields have been underetched on a width of 2 µm, serving as elastic substrates. The residuary area of the 10–30 µm wide fields is based on the thick AlGaAs spacer layer and is free to relax laterally in order to reduce strain in layers, which are grown above it. We have overgrown such elastic fields. A 50 nm thin GaAs buffer and 750 nm ZnSe (overcritical) were deposited under standard MBE conditions. With an optimised mask preparation defects due to leavings on the mask (as those observed in Fig. 4) could be avoided. Results obtained by means of high-resolution X-ray diffraction (HRXRD) indicate that the thick ZnSe layer on the elastic mask is only partially relaxed. The degree of plastic relaxation is only $\gamma = 0.53$. Additionally a triangle shaped diffuse scattering signal is observed in the 115 reciprocal space maps. This is probably due to the existence of pseudomorphic

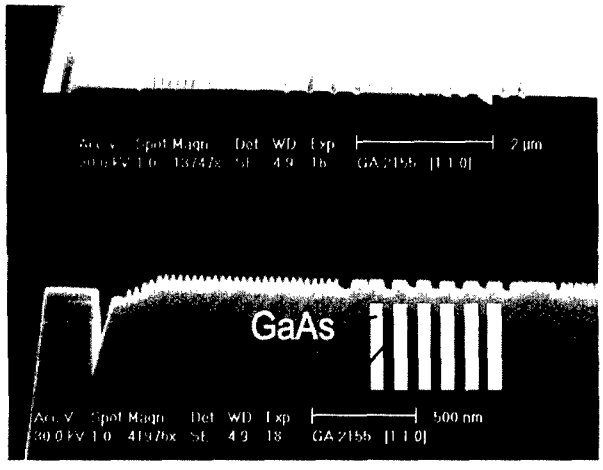

Fig. 6. Scanning electron micrographs from selectively etched AlGaAs/GaAs-superlattices.

fields, which are free of treading dislocations (see Fig. 5). Evaluation of cathodoluminescence micrographs shows a significant reduction of the defect density with the size of the fields. On most of the small fields (edge lengths >10 μm) no defects have been found.

3.2. Analogy to cleaved edge overgrowth

The second mask concept (see Fig. 1d) is analogous to cleaved edge overgrowth (CEO). GaAs/AlGaAs superlattices (SLs) were cleaved and subsequently dipped in hydro-fluoric acid (HF). This selectively etches the AlGaAs layers, and leaves free-standing GaAs lines (see Fig. 6). The smallest line widths realised in this way are as small as 10 nm (35 nm high). The idea is to overgrow these pattern-lines (the combined use of shadow techniques is optional). Since two MBE processes define thickness and width, it should be possible to realise homogeneous nanowires in this way. In contrast to CEO in situ cleaving is not required since the growth area is spatially separated from aluminium–composite layers. In the first experiments we have overgrown such pre-patterned cleave edges with III–V materials (see Fig. 7). Self-assembly of smooth facets has been observed when the nominal thickness of grown layers was of the order of the width of the GaAs-stripes (Fig. 7b). With only thin GaAs/InGaAs layers deposited onto the mask the homogeneity of the etched GaAs-lines was not affected (Fig. 7a). In order to reproducibly realise homogeneous nanowires with this mask concept improved processes for the preparation of the terminated [110] GaAs interfaces (oxide-, or hydrogen-), and for a proper desorption (substrate temperature is critical) have to be developed.

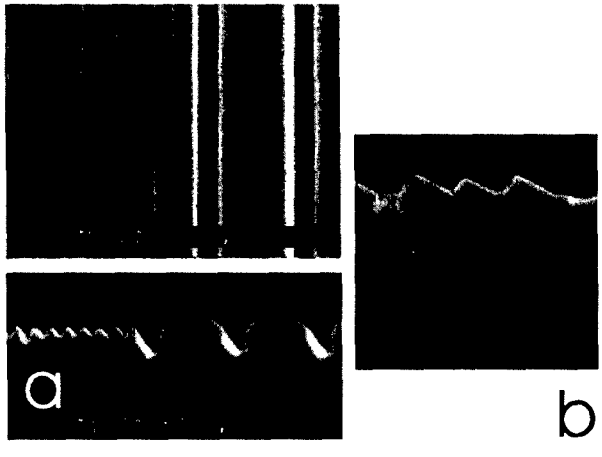

Fig. 7. Scanning electron micrograph of overgrown etched superlattices. (a) Thin layers. (b) Thick layer.

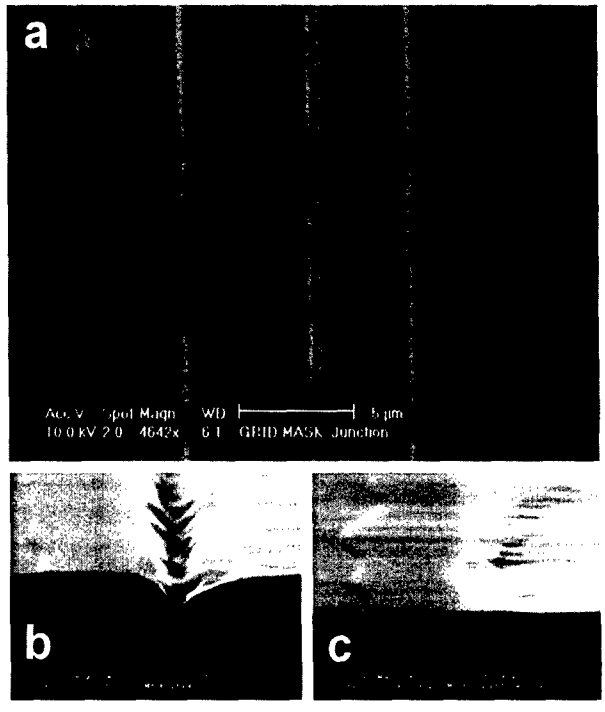

Fig. 8. (a) Scanning electron micrographs from AlGaAs and GaAs stripes, which have been deposited through a 10 μm periodic grid mask with 4.6 μm apertures. (b) A groove between the AlGaAs and the GaAs stripe. (c) Widened apertures level the groove, and coherent periodic arrays of stripes are realised.

3.3. Grid mask

The final mask concept (see Fig. 1c) presented in this contribution is a real two-dimensional mask. A grid mask was structured by etching arrays of aperture stripes (4.5–5.5 μm×150 μm) with 10 μm lateral periodicity into the 1-μm-thick GaAs cap layer. Finally the residual GaAs grid was completely underetched. In this way large areas of the substrate are uncovered, with only the free hanging grid above them. Bending of the grid stripes due to gravity is small. In a first experiment we

have deposited AlGaAs and GaAs layers through the grid with absolute layer offsets of 2.5 μm, and −2.5 μm, respectively (see Fig. 8a). Consequently the growth areas meet in the middle of the aperture lines and in the centre below the free-hanging GaAs grid lines. Dependent on the width of the aperture-lines separate stripes (with grooves; see Fig. 8b), and alternatively interconnected structures with lateral periodicity of 10 μm have been realised (see Fig. 8c). The potential of grid masks is the possibility to perform in situ structuring of lateral-periodic structures with the same many degrees of freedoms that have been discussed above.

4. Conclusion

In summary, directed shadow growth through stationary shadow masks is an in situ technique suited for nanostructuring. Since its high resolution is based on weak diffusion dynamics it addresses especially those materials, which are not well suited for self-assembling techniques. These are LT:III–V (important magnetic semiconductors) and most II-VI semiconductors (group VI-rich growth). We have developed several techniques, which make up the many degrees of freedom of this technique. These are lateral layer offset, size-control, (selective doping,) secondary shadowing, and composition modifications. By this growth of complex nanostructures in three dimensions is realised. Shadow growth also avoids restrictions, which are due to layer-by-layer growth. Therefore unusual materials combinations (e.g. relaxed with pseudomorphic structures) and new devices can be realised.

We have discussed restrictions due to the MBE chamber geometry as the angular spread of the molecular beams, the fixed arrangement of effusion cells, and variations of the fluxes. Possible solutions for these problems have been presented.

Three novel mask concepts were presented. Homogeneous quantum-wires can be realised by overgrowing selectively etched superlattices. In contrary to CEO in situ cleaving is not required. Secondly we have demonstrated that overgrowing elastic masks increases critical thicknesses. Finally we have presented a first two-dimensional stationary shadow mask, the grid mask. This enables the growth of interconnected structures with lateral periodicity.

Acknowledgments

This work is granted by the 'Deutsche Forschungsgemeinschaft' (SFB 410, project A1).

References

[1] D.C. Streit, T.R. Block, A. Han, M. Wojtowicz, D.K. Umemoto, K. Kobayashi, A.K. Oki, P. Liu, R. Lai, G.I. Ng, J. Vac. Sci. Technol. B 13 (1995) 771.
[2] X. Wu, K.H. Gulden, M. Thomas, G. Wilson, J. Walker, G.H. Döhler, J.R. Whinnery, J.S. Smith, J. Cryst. Growth 127 (1993) 896.
[3] A. Lorke, J.H. English, A.C. Gossard, P.M. Petroff, J. Appl. Phys. 77 (1995) 3578.
[4] H. Saito, I. Ogura, Y. Sugimoto, K. Kasahara, Appl. Phys. Lett. 66 (1995) 2466.
[5] Y. Luo, A. Cavus, M. Tamargo, J. Wan, F.H. Pollak, J. Vac. Sci. Technol. B 16 (1998) 1312.
[6] W.T. Tsang, M. Ilegems, Appl. Phys. Lett. 31 (1977) 301.
[7] G. Kaminsky, J. Vac. Sci. Technol. B 3 (1985) 741.
[8] W.T. Tsang, A.Y. Cho, Appl. Phys. Lett. 32 (1978) 491.
[9] K.H. Gulden, X. Wu, J.S. Smith, P. Kiesel, A. Höfler, M. Kneissel, P. Riel, G.H. Döhler, Appl. Phys. Lett. 62 (24) (1993) 3180.
[10] G. Hasnain, D. Mars, G.H. Döhler, M. Ogura, J.S. Smith, Appl. Phys. Lett. 51 (1987) 832.
[11] S. Gundel, Doctoral Dissertation, Physikalisches Institut, Universität Würzburg, 2001.
[12] T. Schallenberg, C. Schumacher, W. Faschinger, Physica E, Proc. MSS 10 (2001).
[13] T. Schallenberg, M. Obert, G. Bacher, V. Türck, C. Schumacher, W. Faschinger, in press.
[14] T. Schallenberg, V. Türck, C. Schumacher, W. Faschinger, in press.
[15] Y.H. Lo, Appl. Phys. Lett. 59 (1991) 2311.
[16] S.C. Jain, A.H. Harker, A. Atkinson, K. Pinardi, J. Appl. Phys. 78 (1995) 1630.